

Program package for multicanonical simulations of U(1) lattice gauge theory

Alexei Bazavov^a and Bernd A. Berg^b

^aDepartment of Physics, University of Arizona, Tucson, Arizona 85721

^bDepartment of Physics, Florida State University, Tallahassee, Florida 32306

Abstract

We document our Fortran 77 code for multicanonical simulations of 4D U(1) lattice gauge theory in the neighborhood of its phase transition. This includes programs and routines for canonical simulations using biased Metropolis heatbath updating and overrelaxation, determination of multicanonical weights via a Wang-Landau recursion, and multicanonical simulations with fixed weights supplemented by overrelaxation sweeps. Measurements are performed for the action, Polyakov loops and some of their structure factors. Many features of the code transcend the particular application and are expected to be useful for other lattice gauge theory models as well as for systems in statistical physics.

Program Summary

Program title: STMC_U1MUCA

Program obtainable from: Temporarily from URL <http://www.hep.fsu.edu/~berg/research>.

Distribution format: tar.gz

Programming language: Fortran 77

Computer: Any capable of compiling and executing Fortran code.

Operating system: Any capable of compiling and executing Fortran code.

Nature of problem: Efficient Markov chain Monte Carlo simulation of U(1) lattice gauge theory close to its phase transition. Measurements and analysis of the action per plaquette, the specific heat, Polyakov loops and their structure factors.

Solution method: Multicanonical simulations with an initial Wang-Landau recursion to determine suitable weight factors. Reweighting to physical values using logarithmic coding and calculating jackknife error bars.

Running time: The prepared tests runs took up to 74 minutes to execute on a 2GHz PC.

Key words: Markov Chain Monte Carlo, Multicanonical, Wang-Landau Recursion, Fortran, Lattice gauge theory, U(1) gauge group.

PACS: 02.70.-c, 11.15.Ha

1. Introduction

Continuum, quantum gauge theories are defined by their Lagrangian densities, which are functions of fields living in 4D Minkowski space-time. In the path-integral representation physical observables are averages over possible field configurations weighted with an exponential factor depending on the action. By performing a Wick rotation to imaginary time the Minkowski metric becomes Euclidean. Discretization of this 4D Euclidean space results in lattice gauge theory (LGT) – a regularization of the original continuum theory, which allows to address non-perturbative problems. For a textbook see, for instance, Ref. [1]. Physical results are recovered in the quantum continuum limit $a \rightarrow 0$, where a is the lattice spacing measured in units proportional to a diverging correlation length.

U(1) pure gauge theory, originally introduced by Wilson [2], is a simple 4D LGT. Nevertheless, determining its phase structure beyond reasonable doubt has turned out to be a non-trivial computational task. One encounters a phase transition which is believed to be first-order on symmetric N_s^4 lattices, e.g. [3, 4, 5]. For a finite temperature $N_s^3 \times N_\tau$, $N_\tau < N_s$ geometry the situ-

ation is less clear: Either second-order for small N_τ and first-order for large N_τ [6], or always second order, possibly corresponding to a novel renormalization group fixed point [7]. In 3D U(1) gauge theory is confining for all values of the coupling on symmetric N_s^3 lattices [8, 9], while in the finite temperature $N_s^2 \times N_\tau$, $N_\tau < N_s$ geometry a deconfining transition of Berezinsky-Kosterlitz-Thouless type [10, 11] is expected, see [12] for recent numerical studies.

In lattice gauge theory one can evaluate Euclidean path integrals stochastically by generating an ensemble of field configurations with Markov chain Monte Carlo (MCMC). In this paper we report MCMC techniques we used in [7]. They are based on multicanonical (MUCA) simulations [13, 14] supplemented by a Wang-Landau (WL) recursion [15], both employed in continuum formulations. For updating we use the biased Metropolis heatbath algorithm (BMHA) of [16] added by overrelaxation [17]. Observables include the specific heat, Polyakov loops and their structure factors (SFs) for low-lying momenta. For the analysis of these data binning is used to render auto-correlations negligible and a logarithmically coded reweighting

procedure calculates averages with jackknife error bars.

Our program package

STMC_U1MUCA.tgz

can be downloaded from the web at

<http://www.hep.fsu.edu/~berg/research> .

Unfolding of STMC_U1MUCA.tgz with `tar -zxvf` creates a tree structure with root directory STMC_U1MUCA. Folders on the first level are ExampleRuns, ForProg and Libs. Besides in the subfolders of ExampleRuns, copies of all main programs are found in ForProg. Fortran functions and subroutines of our code are located in the subfolders of Libs, which are Fortran, Fortran_par, U1, and U1_par. Routines in Fortran and U1 are modular, so that they can be called in any Fortran program, while routines in the other two subfolders need user defined parameter files, which they include at compilation. General purpose routines are in the Fortran subfolders and to a large extent taken over from ForLib of [14], while routines specialized to U(1) are in the U1 folders. Parameter files are

$$\text{bmha.par, lat.par, lat.dat, mc.par} \quad (1)$$

for canonical simulations and in addition

$$\text{sf.par, u1muca.par} \quad (2)$$

for SF measurements and MUCA simulations with WL recursion. The main programs and the routines of the subfolders Fortran_par and U1_par include common blocks when needed. These common blocks with names `common*.f` are also located in the Fortran_par and U1_par subfolders.

This paper is organized as follows. In Sec. 2 we define U(1) LGT and introduce the routines for our BMHA and for measurements of some observables. Sec. 3 is devoted to our code for MUCA runs and to the analysis of these data. Sections 2 and 3 both finish with explicit example runs, where Sec. 3 uses on input action parameter estimates obtained in Sec. 2. A brief summary and conclusions are given in the final section 4.

2. Canonical simulations

Our code is written for a variable dimension d and supposed to work for $d \geq 2$. However, its use has mainly been confined to $d = 4$ to which we restrict most of the subsequent discussion.

After U(1) gauge theory is discretized its fundamental degrees of freedom reside on the links of a 4D hypercubic lattice which we label by x, μ : x is a 4D vector giving the location of a site, and $\mu = 1, 2, 3, 4$ is the direction of the link originating from this site, $\mu = 4$ corresponds to the temporal direction of extension N_τ and $\mu = 1, 2, 3$ to the spatial directions of extension N_s .

The system contains $N_s^3 \times N_\tau$ sites and $N_s^3 \times N_\tau \times 4$ degrees of freedom $U_{x,\mu}$ that belong to U(1) gauge group, which we parametrize by

$$U_{x,\mu} = \exp(i\theta_{x,\mu}), \quad \theta_{x,\mu} \in [0, 2\pi). \quad (3)$$

In our code we use Wilson's action

$$S = \sum_x \sum_{\mu=1}^4 \sum_{\nu < \mu} \text{Re}(U_{x,\mu} U_{x+\hat{\mu},\nu} U_{x+\hat{\nu},\mu}^+ U_{x,\nu}^+). \quad (4)$$

The product $U_{x,\mu} U_{x+\hat{\mu},\nu} U_{x+\hat{\nu},\mu}^+ U_{x,\nu}^+$ is taken around a *plaquette*, an elementary square of the lattice. In 4D each link participates in 6 plaquettes ($2(d-1)$ in d -dimension). Products such as $U_{x+\hat{\mu},\nu} U_{x+\hat{\nu},\mu}^+ U_{x,\nu}^+$ are called *staples*.

In canonical simulations one generates an ensemble of configurations weighted with $\exp(\beta S)$, the Boltzmann factor of a system with energy $-S$, which is in contact with a heatbath at inverse temperature β . Here β is the inverse temperature of a statistical mechanics on the lattice and not the physical temperature of the LGT. The latter is given by the temporal extent of the lattice: $T = 1/(aN_\tau)$.

An important property of the action (4) is *locality*: For a link update only its interaction with a small set of neighbors is needed. The part of the action involving a link $U_{x,\mu}$ being updated (with all other links frozen) is:

$$S(U_{x,\mu}) = \text{Re} \left\{ U_{x,\mu} \left[\sum_{\nu \neq \mu} U_{x+\hat{\mu},\nu} U_{x+\hat{\nu},\mu}^+ U_{x,\nu}^+ + \sum_{\nu \neq \mu} U_{x+\hat{\mu}-\hat{\nu},\nu} U_{x-\hat{\nu},\mu}^+ U_{x-\hat{\nu},\nu} \right] \right\}. \quad (5)$$

The sum in square brackets [...] runs over 6 staples and is evaluated before updating the link. We denote it

$$U_\square = \alpha \exp(i\theta_\square) = \left[\sum_{\nu \neq \mu} U_{x+\hat{\mu},\nu} U_{x+\hat{\nu},\mu}^+ U_{x,\nu}^+ + U_{x+\hat{\mu}-\hat{\nu},\nu} U_{x-\hat{\nu},\mu}^+ U_{x-\hat{\nu},\nu} \right]. \quad (6)$$

To simplify the notation we drop the x, μ subscripts of the link:

$$S(U) \sim \text{Re}(UU_\square). \quad (7)$$

Thus the distribution

$$P(U) \sim e^{\beta S} = e^{\beta \text{Re}(UU_\square)} \quad (8)$$

needs to be sampled. In angular variables

$$\text{Re}(UU_\square) = \alpha \text{Re}(e^{i(\theta+\theta_\square)}) = \alpha \cos(\theta + \theta_\square) \quad (9)$$

and

$$P(\theta)d\theta \sim e^{\beta \alpha \cos(\theta+\theta_\square)} d\theta = e^{\beta \alpha \cos(\varphi)} d\varphi, \quad \varphi = \theta + \theta_\square.$$

The final probability density function (PDF) is

$$P(\alpha; \varphi) \sim e^{\beta \alpha \cos \varphi}. \quad (10)$$

It is straightforward to implement the Metropolis algorithm [18] for (10). A value φ_{new} is proposed uniformly in the interval $[0, 2\pi)$ and then accepted with probability

$$\min \left\{ 1, \frac{P(\alpha; \varphi_{new})}{P(\alpha; \varphi_{old})} \right\}. \quad (11)$$

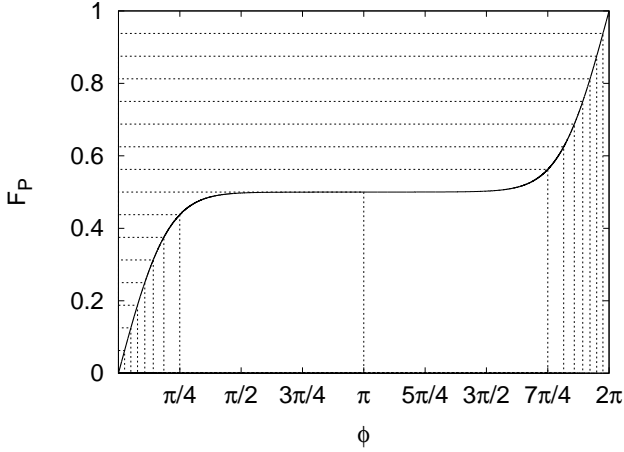


Figure 1: The cumulative distribution function $F_P(\alpha = 3.9375; \varphi)$ for an arbitrarily chosen value of the parameter α .

However, it has low acceptance rate in the region of interest ($0.8 \leq \beta \leq 1.2$). An efficient heatbath algorithm (HBA) is hard to design since the cumulative distribution function (CDF)

$$F_P(\alpha; \varphi) = \frac{\int_0^\varphi P(\alpha; \varphi') d\varphi'}{\int_0^{2\pi} P(\alpha; \varphi') d\varphi'} \quad (12)$$

is not easily invertible, because it cannot be represented in terms of elementary functions. Nevertheless, two variations of heatbath algorithms for U(1) do exist [19], [20].

2.1. Biased Metropolis heatbath algorithm

The MCMC updating of our code relies on a BMHA [16], which approximates heatbath probabilities by tables as described in the following. The updating variable φ is drawn from some distribution $Q(\alpha; \varphi)$ and then accepted with probability

$$\min \left\{ 1, \frac{P(\alpha; \varphi_{new})}{P(\alpha; \varphi_{old})} \frac{Q(\alpha; \varphi_{old})}{Q(\alpha; \varphi_{new})} \right\}. \quad (13)$$

This turns out to be a special case of general acceptance probabilities introduced by Hastings [21]. One refers to the proposals as *biased* when $Q(\alpha; \varphi_{old})/Q(\alpha; \varphi_{new}) \neq 1$ holds.

For the heatbath algorithm the proposal probability $Q(\alpha; \varphi)$ is chosen to be identical to the target distribution $P(\alpha; \varphi)$, so that φ_{new} is always accepted. In practice it is sufficient that $Q(\alpha; \varphi)$ is a good approximation of $P(\alpha; \varphi)$. We approximate the CDF (12) by a piece-wise linear function $F_Q(\alpha; \varphi)$. Compare Fig. 1 and Fig. 2. We partition the F_Q axis into n equidistant pieces ($n = 16$ in the figures), which defines $\varphi^1, \dots, \varphi^n$ values via the relation $F_Q(\alpha; \varphi^j) - F_Q(\alpha; \varphi^{j-1}) = 1/n$, and we call an interval $(\varphi^{j-1}, \varphi^j]$ a bin. The approximated PDF

$$Q(\alpha; \varphi) = \frac{dF_Q}{d\varphi} = \frac{1}{n(\varphi^j - \varphi^{j-1})} = \frac{1}{n\Delta\varphi^j} \quad (14)$$

is flat in each bin and it is easy to generate φ from $Q(\alpha; \varphi)$: One first picks a bin j with uniform probability ($1/n$) and then generates φ uniformly in this bin.

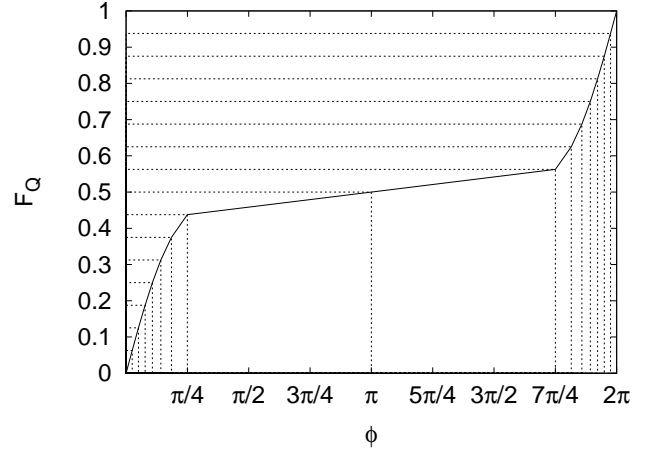


Figure 2: The cumulative distribution function $F_Q(\alpha = 3.9375; \varphi)$ which serves as an approximation of F_P . Compare to Fig. 1.

We call this scheme BMHA because a Metropolis accept/reject step is used and a bias is introduced to enhance the acceptance rate by making the proposal probability an approximation of the one of the heatbath algorithm. When the discretization step goes to zero

$$\frac{\Delta\varphi^{j_{new}}}{\Delta\varphi^{j_{old}}} \rightarrow \frac{1/P(\alpha; \varphi_{new})}{1/P(\alpha; \varphi_{old})} = \frac{P(\alpha; \varphi_{old})}{P(\alpha; \varphi_{new})} \quad (15)$$

follows from (14) and the acceptance rate (13) approaches 1.

$P(\alpha; \varphi)$ depends on an external parameter $0 \leq \alpha \leq \alpha_{max} = 2(d-1)$ and the inverse temperature β . We discretize α for the proposal probability $Q(\alpha; \varphi)$. Before updating a link in the code we evaluate the sum of the staples U_\square and decompose it into the magnitude α and phase θ_\square . At this stage α is then known.

The following is a summary of the algorithm we use to generate the φ variable with the PDF (10). These routines are located in `Libs/U1_par`.

2.1.1. Table generation

1. Choose m bins for the parameter axis α and n bins for the variable φ . Two $m \times n$ arrays are needed. We take m and n to be powers of 2, because n being a power of 2 speeds up finding j_{old} (20), though m can, in principle, be arbitrary.
2. Calculate a discrete set of α values by

$$\alpha^i = \left(i - \frac{1}{2} \right) \frac{\alpha_{max}}{m}, \quad i = 1, \dots, m. \quad (16)$$

3. For each α^i evaluate

$$F_Q^i(\varphi) = \frac{\int_0^\varphi P(\alpha^i; \varphi') d\varphi'}{\int_0^{2\pi} P(\alpha^i; \varphi') d\varphi'} \quad (17)$$

by numerical integration with $\beta = \text{beta_table}$ as set in `mc.par`. The inverse temperature of the canonical simulation is denoted `beta` in the code. We reserve the possibility to have different values of the inverse temperature for the BMHA table generation and for the simulation. Of course,

for `beta_table = beta` the table approximates the heatbath distribution at `beta`. When a range of inverse temperatures is used, as in MUCA simulations, one can tune the acceptance rate by playing with `beta_table`. The ranges that we used in multicanonical runs were narrow, so we were content with setting `beta_table = bmax`.

4. Tabulate $F_Q^i(\varphi)$ by values $\varphi^{i,j}$ defined by

$$\frac{j}{n} = F_Q^i(\varphi^{i,j}) \Leftrightarrow \varphi^{i,j} = (F_Q^i)^{-1}\left(\frac{j}{n}\right) \quad (18)$$

and the differences

$$\Delta\varphi^{i,j} = \varphi^{i,j} - \varphi^{i,j-1}. \quad (19)$$

The common block `common_bmhatable.f`, which is listed below, stores the quantities $\varphi^{i,j}$, $\Delta\varphi^{i,j}$ and $\ln \Delta\varphi^{i,j}$, respectively:

C Table for BMHA.

```
common/tabbma/ tabbm(nbm2,nbm1),
& delbm(nbm2,nbm1), dbmln(nbm2,nbm1)
```

where the parameters `nbm1 = m` and `nbm2 = n` are set in the file `bmha.par`:

c Biased Metropolis-HeatBath (BMHA) parameters:

```
parameter(nbm1=2**5,
& n2log2=7,nbm2=2**n2log2)
```

2.1.2. BMH updating

Our implementation of BMH updates is given in the routine `u1_bmha.f`. A call to `u1_bmha.f` performs one *sweep*, which here is defined by updating each variable (U(1) matrix) once in sequential order. For each, single BMH update it calls the subroutine `u1_bmha_update.f`. Its functions are shortly described in the following.

1. After α and θ_\perp are calculated by the `u1_getstaple` subroutine, determine the α bin $k = \text{Int}[\alpha/\alpha_{max}] + 1$, where $\text{Int}[x]$ denotes rounding to the largest integer $\leq x$.
2. For given k determine to which bin the previous value $\varphi_{old} = (\theta_{old} + \theta_\perp) \bmod 2\pi$ belongs (in the code θ_{old} value is stored in `aphase` array). This is done with a binary search

$$j_{old} \rightarrow j_{old} + 2^i \cdot \text{sign}(\varphi - \varphi^{i,j_{old}}), \quad i \rightarrow i - 1 \quad (20)$$

starting with $j_{old} = 0$, $i = \log_2 n - 1$.

3. Pick a new bin

$$j_{new} = \text{Int}[nr_1] + 1, \quad (21)$$

where r_1 is a uniform random number in $[0,1)$.

4. Pick a new value

$$\varphi_{new} = \varphi^{i,j_{new}} - \Delta\varphi^{i,j_{new}} r_2, \quad (22)$$

where r_2 is a uniform random number in $[0,1)$.

5. Accept φ_{new} with probability (13).
6. If accepted, store $\theta_{new} = (2\pi + \varphi_{new} - \theta_\perp) \bmod 2\pi$ in the `aphase` array.

For U(1) and SU(2) we found [16] that $m = 32$ and $n = 128$ are large enough to achieve ~ 0.97 acceptance rate. Thus, the BMHA achieves practically heatbath efficiency. It becomes important for cases where a conventional HBA is difficult to implement and/or computationally inefficient.

2.2. Overrelaxation

We use overrelaxation (OR) to faster decorrelate the system. OR algorithms were introduced by Adler. See [22] and references given therein. In the formulation of Ref. [23] the idea is to generate a new value of the link matrix that lies as far as possible away from the old value without changing the action too much. This is done by reflecting the old matrix about the link matrix, which maximizes the action locally. In U(1) LGT one reflects θ_{old} about the element θ_0 , which maximizes the PDF (10). The φ value that maximizes (10) is $\varphi_0 = \theta_0 + \theta_\perp$. Reflecting θ_{old} about $\theta_0 = -\theta_\perp$ we find

$$\theta_{new} = \theta_0 - (\theta_{old} - \theta_0) = -2\theta_\perp - \theta_{old}. \quad (23)$$

As θ_{new} (23) does not change the action, OR constitutes in our case a *microcanonical* update. Our implementation is the subroutine `u1_over.f`, which performs one overrelaxation sweep. In the code $\theta_{new} = (6\pi - 2\theta_\perp - \theta_{old}) \bmod 2\pi$.

2.3. Example runs

Short canonical simulations are needed to determine the action range for the multicanonical runs. We perform 1 BMHA sweep followed by 2 OR sweeps. Runs in 3D on $6^2 \times 4$ lattices are prepared in the subfolders

`C3D04t06xb1p0` and `C3D04t06xb2p0`

of the folder `ExampleRuns` and in 4D on $6^3 \times 4$ lattices in

`C4D04t06xb0p9` and `C4D04t06xb1p1`.

Parameters are set in the `*.par` and `lat.dat` files, the lattice size in `lat.par` and `lat.dat`: Run parameters in `mc.par` and the BMHA table size in `bmha.par`, which is kept the same for all runs.

The general structure of our MCMC simulations is that outlined in [14]: Lattice set-up and initialization are done by the routine `u1_init.f` followed by `nequi` sweeps for equilibration, which do not record measurements. Afterwards `nrpt` \times `nmeas` measurements are carried out, each after `nsw` sweeps (in [14] only `nsw = 1`).

The 4D β values embrace the pseudo-transition region of the $6^3 \times 4$ lattice: $\beta = 0.9$ in the disordered and $\beta = 1.1$ in the ordered phase. To avoid divergence of the equilibration time with increasing lattice size, the start configuration has to match the phase: Ordered (`istart = 1`) in the ordered and disordered (`istart = 2`) in the disordered phase.

The production program has to be compiled with

```
../make77 u1_tsbmho.f
```

where the `make77` file is located one level up in the tree. Besides Fortran 77 compilation the `make77` moves parameter files around, so that they are properly included by subroutines, which need them. The Fortran compiler defined in our `make77` is `g77`. You may have to replace it with the one used on your computing platform. In the `tcshell` CPU times are recorded by running the `a.out` executable with

```
../CPUtime > & fln.txt &
```

in the background, where the file `CPUtime` is also located one level up in the tree. While running one can monitor the progress by looking up the `progress.d` file. In test runs on a Intel E5405 2 GHz quad-core PC using `g77` version 3.4.6 (Red Hat 3.4.6-4) the execution times for the prepared simulations were 3m35s in 4D and 41s in 3D.

After a production run `ana_ts1u1.f` is used to analyze the action data. In the present context we only need the mean action values as input for the action ranges set in our multicanonical runs. With `gnuplot h01.plt` or `i01.plt` one plots the action histogram. The BMHA acceptance rate is also returned by `ana_ts1u1.f`. Further, the integrated autocorrelation length τ_{int} is estimated, but the statistics may not always be sufficiently large for a good determination (the statistics needed to estimate the average action is much smaller [14]). The relevant parameters for calculating τ_{int} have to be set in the analysis program and a plot is obtained with `gnuplot a1tau.plt`.

As rounding errors in floating point operations depend on the compiler, the actual numbers obtained for the average action on different computing platforms may vary within statistical errors. In our 4D run they were

$$\text{actm}/n_p = 0.46942 (18) \text{ at } \beta = 0.9, \quad (24)$$

$$\text{actm}/n_p = 0.71728 (14) \text{ at } \beta = 1.1, \quad (25)$$

where n_p is the number of plaquettes. Approximated, this range across the phase transition will be used in the `u1muca.par` file of our subsequent MUCA simulation:

$$\text{actmin} = S_{\min} = \text{actm} \text{ at } \beta_{\min} = 0.9, \quad (26)$$

$$\text{actmax} = S_{\max} = \text{actm} \text{ at } \beta_{\max} = 1.1. \quad (27)$$

The procedure for running 3D examples is the same as for the 4D runs described above. To cover the pseudo-transition region on $6^2 \times 4$ lattice we set the inverse temperatures for the canonical runs at $\beta = 1.0$ in the disordered and $\beta = 2.0$ in the ordered phase. The choice of a broader range of temperatures is appropriate, related to finite size effects that scale logarithmically with the lattice size. Average action values obtained are

$$\text{actm}/n_p = 0.47495 (27) \text{ at } \beta = 1.0, \quad (28)$$

$$\text{actm}/n_p = 0.81079 (15) \text{ at } \beta = 2.0. \quad (29)$$

3. Multicanonical simulations

In MUCA [13] simulations one samples the phase space with weights, which are a *working estimate* [14] of the inverse spectral density up to an overall factor. This makes the energy histogram approximately flat and allows for efficient reconstruction of canonical expectation values in a range of temperatures ($\beta_{\min}, \beta_{\max}$). This has many applications and is especially useful when studying the vicinity of first-order phase transitions, where canonical histograms exhibit a double-peak structure, suppressing tunneling between phases even for relatively small-sized system (e.g., see [24] for a recent study of 3D Potts models). For second-order phase transitions the usefulness of

MUCA simulations has been discussed in the context of cluster algorithms [25]. Most important and successful applications target complex systems like, for instance, biomolecules [26].

The MUCA method consists of two parts [14]: A recursion to determine the weights and a simulation with frozen weights. For the first part we have programmed a continuous version of the WL recursion [15].

3.1. Wang-Landau recursion

Because the WL code of this section is programmed for generic use in statistical physics systems we use the energy E instead of the action notation. In earlier recursions for MUCA parameters (see, e.g., [14]) one was iterating with a weight function of the energy, $w(E)$, inversely proportional to the number of histogram entries at E . In contrast to that the WL algorithm [15] increments the weight multiplicatively, i.e., additively in logarithmic coding:

$$\ln w(E'') \rightarrow \ln w(E'') - a_{WL}, \quad a_{WL} > 0 \quad (30)$$

at every WL update attempt $E \rightarrow E'$, where $\text{addwl} = a_{WL}$ in our code. Here $E'' = E$ when the update is rejected and $E'' = E'$ when the update is accepted. After a sufficiently flat histogram is sampled (we come back to this point), the WL parameter is refined,

$$a_{WL} \rightarrow a_{WL}/2. \quad (31)$$

In its original version the WL algorithm deals with discrete systems like Ising or Potts models for which histogram entries correspond naturally to the discrete values of the energy. However, for continuous systems binsizes are free parameters and we have to deal with their tuning.

We discretize the U(1) action range into bins of a size large enough in ΔS , so that one update cannot jump over a bin. Here $\Delta S < 4(d-1)$, because there are $2(d-1)$ plaquettes attached to a link and the range of the plaquette action is in the interval $[-1, +1]$, which gives another factor 2. In the program this value ΔS is defined as `delE`. Next, we are *not* using constant weights over each bin, but instead a constant temperature interpolation as already suggested in [13].

One WL update has two parts:

1. A MUCA update of the energy (in our U(1) code action) using the weights at hand.
2. A WL update (30) of the MUCA weights.

In our code a WL sweep is done by a call to

$$\text{u1_mucabmha.f}, \quad (32)$$

which updates link variables in sequential order through calls to the included routine `u1_update_mubmha.f`. This routine generalizes BMH updating to the situation of MUCA weights, which is relatively straightforward (see the code for details) and increases efficiency compared to MUCA Metropolis simulations by a factor 3 to 5. It calls three modularly coded routines: The functions `fmuca1n.f` and `betax.f` to calculate weights and β values as needed for the BMHA. After an action update

is done, the WL update (30) is performed by a call to the sub-routine `wala_updt.f`, which is at the heart of our modifications of the WL algorithm.

The basic point is that `wala_updt.f` does not only iterate the number of histogram entries, but also the mean value within each histogram bin. The relevant lines of that code are listed below.

```
C Put addwl <= zero in 2. part of MUCA.
  if(addwl.gt.zero) then
    wln(ix)=wln(ix)-addwl
    xwl(ix)=(hx(ix)*xwl(ix)+x)
  endif
  hx(ix)=hx(ix)+one
  hx0(ix)=hx0(ix)+one
  if(addwl.gt.zero) then
    xwl(ix)=xwl(ix)/hx(ix)
  else
    xmu(ix)=xmu(ix)+x
  endif
```

Besides performing the update (30) the routine tracks the histogram entries in the array `hx` and for `addwl > 0` the mean value of `x` within bin `ix` as `xwl(ix)`. For `addwl ≤ 0` MUCA simulations with fixed weights are performed. Then the `xwl(ix)` values are kept constant, but the array `xmu` allows one to calculate at a later stage the average within a histogram bin.

The `xwl(ix)` values are essential entries for the Fortran functions `fmuca.f` and `betax.f`. Logarithmic WL weights `wln(ix)` correspond to the mean value positions. For general `x` values the function `fmucaln.f` interpolates the logarithmic weights linearly from the `wln(ix)` weights of the two neighboring mean values:

```
x=(E-Emin)/dele
ix=1+int(x)
if(x.gt.xwl(1).and.x.lt.xwl(ixmax)) then
  if(x.gt.xwl(ix)) then
    ix1=ix+1
  else
    ix1=ix-1
  endif
  w1=abs(xwl(ix1)-x)
  w2=abs(xwl(ix)-x)
  fmucaln=(w1*wln(ix)+w2*wln(ix1))/(w1+w2)
elseif(x.le.xwl(1)) then ...
```

With this input the function `betax` calculates the β values used by the BMHA:

```
if(x.le.xwl(ix)) then
  if(ix.eq.1) then
    betax=bmax
  else
    betax=(wln(ix-1)-wln(ix))/
&      (xwl(ix)-xwl(ix-1))/dele
  endif
else
  if(ix.eq.ixmax) then
```

```
    betax=bmin
  else
    betax=(wln(ix)-wln(ix+1))/
&      (xwl(ix+1)-xwl(ix))/dele
  endif
endif
```

Although these routines are modular, to transfer the relevant arrays and variables into the U(1) code, they are all kept in the common block `common_u1muca.f`.

```
C wln      MUCA logarithmic weights (w=exp(wln)).
C hx      Total count of histogram entries.
C hx0     For reconstruction of entries during
C         one recursion segment.
C xwl     Continuously updated mean values of
C         histogram bins
C         (used with MUCA weights).
C xmu     Keeps track of mean values of
C         histogram bins during
C         fixed weights MUCA runs.
C addwl   Wang-Landau parameter.
C flat    Flatness of the histogram as measured
C         by hist_flat.f.
C irup1   Start of WL recursion loop.
C irec    Number of WL recursions done.
C mucarun Number of MUCA run
C         (0 for WL recursion, then 1, 2, ...).
C ntun    Number of tunneling (cycling) events.
C ltun0   Logical used when incrementing ntun.
&      common/wln/wln(ixmax),hx(ixmax),
&      hx0(ixmax),xwl(ixmax),addwl,xmu(ixmax),
&      flat,irup1,irec,mucarun,ntun,ltun0
```

The common block is on the specialized U(1) level, because the array dimension

$$ixmax = \text{Int}[(actmax - actmin)(np/(4(nd - 1)))]$$

depends on the number `np` of plaquettes of the U(1) lattice. The relevant parameters are set by the user in `u1muca.par`.

Once the system cycled from the minimum (26) to the maximum (27) action value and back

$$actmin \longleftrightarrow actmax, \quad (33)$$

a WL recursion (31) is attempted. The *cycling* or *tunneling* condition (33) ensures that the range of interest has indeed been covered. In addition we require that the sampled action histogram is sufficiently flat. The flatness is defined by

$$flatness = h_{min}/h_{max}, \quad (34)$$

where h_{min} and h_{max} are the smallest and largest numbers of histogram entries in the range of interest, and are calculated by our modular routine `hist_flat.f`. Our cut on this quantity is set by `flatcut` in `u1muca.par`. In our simulations [7] we used `flatcut = 0.5`. This is rather weak compared to the requirement in the original WL approach [15] that “the histogram

$H(E)$ for all possible E is not less than 80% of the average histogram $\langle H(E) \rangle$, although their definition of flatness is less stringent than our Eq. (34). The conceptual difference is that the WL paper aims at iterating all the way towards an accurate estimate of the inverse spectral density, while we are content with a working estimate, which enables cycling (33). The estimate of the spectral density is then postponed to our continuation with frozen weight for which convergence of the MCMC process is rigorously proven [14], whereas no such proof exists for the WL algorithm.

It needs to be mentioned that the histogram hx is accumulated over the entire recursion process and the same is true for the refinement of the weights wln . The histogram $hx0$ keeps track of the entries between WL recursions. Presently this information is not used in the code. One may consider to apply a flatness criterion to $hx0$ instead of hx . This is just one of many fine tuning options, which we did not explore, because the WL recursion in its present form took just a few percent of the CPU time in our U(1) simulations [7].

The desired number of WL recursions (31) is set by the parameter $nrec$ of `u1muca.par`, typically $nrec = 20$ or somewhat larger. To achieve this, $nrup$ (number (n) recursions (r) upper (up) limit) WL recursion attempts are allowed, each accommodating up to $nupdt$ WL update sweeps. The update sweeps are interrupted for a recursion attempt when cycling (33) is recorded by our modularly coded subroutine `tuna.cnt.f`, which checks after every sweep. So, $nrup \times nupdt$ is the maximum number of sweeps spent on the WL recursion part. The process is aborted if the given limit is exhausted before $nrec$ WL recursions are completed.

3.2. Fixed weights MUCA simulations and measurements

Fixed weight MUCA simulations are performed by the routines discussed in the previous section, only that the WL update (30) is no longer performed, what is programmed to be the case for $addwl \leq 0$. We still perform updates of the weights in-between (long) MUCA production runs, which is done by a call to `u1mu_rec1.f` in the initialization routine `u1mu_init.f`.

Overall our simulation consists of

$$nequi + nrpt \times nmeas \times nsw$$

BMHA sweeps, each (optionally) supplemented by 2 overrelaxation sweeps. During a MUCA simulation several physical quantities (described below in the section on data analysis) are measured by the `u1sf_measure` subroutine.

Measurements are performed every nsw sweeps and accumulated in the arrays defined in `common_u1.f`:

```
c aphase(nd,ms): Phase of the U(1) "matrix".
c               (We store aphase and
c               the matrix on the link is
c               e^{i aphase}.)
c act:          Energy (action) variable.
c amin,amax:   Action act minimum and
c               maximum of the MC sweep.
c acpt:        Counts accepted updates.
```

```
c tsa:          Time series action array.
c a_min,a_max: Action minimum and maximum for
c               a series of sweeps.
c tsws,tswt:   Time series for lattice
c               average spacelike and timelike
c               Wilson plaquette loops.
c plreal,plimag: Space arrays for Polyakov
c               loops in (nd-1) dimensions.
c tspr,tspi:   Time series for lattice
c               average Polyakov loops.
c isublat:     sublattice for Polyakov loops
c               (in t=0 slice).
               common /u1/ aphase(nd,ms),act,amin,amax,
               & acpt,tsa(nmeas),a_min,a_max,tsws(nmeas),
               & tswt(nmeas),plreal(mxs),plimag(mxs),
               & tspr(nmeas),tspi(nmeas),isublat(mxs)
```

and in `common_sf.f`:

```
C Arrays for structure function measurements.
   common/u1sf/ tssf(ntotalsfbox,nmeas),
   & nsfcomp(1:ntotalsfbox,0:ndimsf)
```

Then each $nmeas \times nsw$ sweeps (i.e., on each iteration of the `nrpt` loop) the arrays with measurements are written on disk by the `u1mu_rw_meas` subroutine, which can also read data. With a call to `u1wl_backup.f` the current state of the lattice is backed up on disk. This allows one to restart the program from the latest iteration of the `nrpt` loop if it gets interrupted and ensures that not more than $1/nrpt$ of the total running time is lost in such a case. Typically, we set $nrpt=32$.

3.3. Data analysis

The program `ana_u1mu.f` calculates action, specific heat and two Polyakov loop susceptibilities, the program `sfana_u1mu.f` Polyakov loop structure factors. Definitions are given in the following with names of corresponding gnuplot driver files in parenthesis. The specific heat (`plot_C.plt`) is

$$C(\beta) = \frac{1}{N_p} [\langle S^2 \rangle - \langle S \rangle^2] \quad \text{with } N_p = \frac{d(d-1)}{2} N_s^3 N_\tau \quad (35)$$

where S is the action (`plot_a.plt`). Besides the action we measure Polyakov loops and their low-momentum structure factors. Polyakov loops $P_{\vec{x}}$ are the U_{ij} products along the straight lines in N_τ direction. For U(1) LGT each $P_{\vec{x}}$ is a complex number on the unit circle and \vec{x} labels the sites of the spatial sublattice. From the sum over all Polyakov loops

$$P = \sum_{\vec{x}} P_{\vec{x}} \quad (36)$$

we find the susceptibility of the absolute value $|P|$

$$\chi_{\max}(\beta) = \frac{1}{N_s^3} [\langle |P|^2 \rangle - \langle |P| \rangle^2] \quad (37)$$

(`plot_CP.plt`), and the susceptibility with respect to β

$$\chi_{\max}^\beta(\beta) = \frac{1}{N_s^3} \frac{d}{d\beta} \langle |P| \rangle \quad (38)$$

(plot_CPb.plt). The analogues in spin system are the magnetic susceptibilities with respect to an external magnetic field and with respect to the temperature.

3.3.1. Structure factors

Structure factors are defined by

$$F(\vec{k}) = \frac{1}{N_s^3} \left\langle \left| \sum_{\vec{x}} P(\vec{x}) \exp(i\vec{k}\vec{x}) \right|^2 \right\rangle, \quad \vec{k} = \frac{2\pi}{N_s} \vec{n}, \quad (39)$$

where \vec{n} is an integer vector to which we refer as momentum in the following (it differs from the structure factor momentum \vec{k} by a constant prefactor) to describe how we average over different momenta.

In `sf.par`

```
C (0,0,1), (0,1,0), (1,0,0), and so on,
C are stored separately.
C ndimsf: number of dimensions for
C the structure function.
C nsfmax: maximum value of
C \vec{n}=(n1,n2,n3,...,n_ndimsf)
C with 0 =< n1,n2,..n_ndimsf =< nsfmax.
C nsfbox: total number of \vec{n} components.
      parameter(ndimsf=nd-1,nsfmax=1,
      & nsfbox=(nsfmax+1)**ndimsf)
```

the dimension `ndimsf` of the sublattice on which SFs are calculated is defined and one sets the maximum value of the components of the momentum, `nsfmax`,

$$\vec{n} = (n_1, n_2, \dots, n_{\text{ndimsf}}), \quad (40)$$

$$n_i = 0, \dots, \text{nsfmax}, \quad i = 1, \dots, \text{ndimsf}. \quad (41)$$

As n_i counting is 0-based we measure during the simulation

$$\text{ntotalsfbox} = (\text{nsfmax} + 1)^{\text{ndimsf}} \quad (42)$$

SF components. Their momenta are stored in the `nsfcomp` array. In the example of a 4D multicanonical run given in the next section `ntotalsfbox`=(1+1)³=8. Initialization of the arrays for structure factor measurements is carried out by the routine `sf_box_init`, which also outputs how momenta are initialized and numbered:

```
sf_box_init: Structure factors initialized:
      ndimsf = 3
      nsfmax = 1
      nsfbox = 8
```

Integer vectors generated:

#	n ²	components....			
1	0	0	0	0	0
2	1	0	0	1	1
3	1	0	1	0	0
4	2	0	1	1	1
5	1	1	0	0	0
6	2	1	0	1	1
7	2	1	1	0	0
8	3	1	1	1	1

`sf_box_init` done.

These eight SFs are measured during this simulation. For a spatially symmetric lattice SF components with permuted momenta, i.e. (0,0,1), (0,1,0) and (1,0,0) are equivalent and there are only

$$\text{nsfdiff} = \frac{(\text{nsfmax} + \text{ndimsf})!}{\text{nsfmax}! \text{ndimsf}!} \quad (43)$$

different modes. In the example `nsfdiff`=4 and they are

$$(0,0,0), (0,0,1), (0,1,1) \text{ and } (1,1,1).$$

To average SFs over permutations of momenta one needs to identify momenta that differ up to permutations, calculate their multiplicity (i.e., the number of permutations) and construct a mapping from all momenta to the set of non-equivalent momenta. For this purpose the `sf_box_shuffle.f` subroutine is used. It returns three arrays corresponding to the elements described above: `nsfcomp_diff`, `nsfmulti`, `nsfmapping`. Using them the analysis program `sfana_u1mu.f` averages SF components and outputs them in files prefixed with the non-equivalent momenta components (for instance, the SF with $\vec{n} = (0,1,1)$ is output in `011sf006x004tmu01.d`). The SF normalization in (39) is defined so that $F(\vec{k}) = 1$ at $\beta = 0$ for all momenta and dimensions. The output of `sf_box_shuffle.f` from our example run is:

`sf_box_shuffle:`

Different SF components (integer vectors):

#	multi	n ²	components....		
1	1	0	0	0	0
2	3	1	0	0	1
3	3	2	0	1	1
4	1	3	1	1	1

Mapping of the components (888 separator):

1	0	0	0	888	1	888	0	0	0
2	0	0	1	888	2	888	0	0	1
3	0	1	0	888	2	888	0	0	1
4	0	1	1	888	3	888	0	1	1
5	1	0	0	888	2	888	0	0	1
6	1	0	1	888	3	888	0	1	1
7	1	1	0	888	3	888	0	1	1
8	1	1	1	888	4	888	1	1	1

`sf_box_shuffle` done.

The first part of the output shows that four different SF components were identified and in the second part the mapping from the eight original momenta is shown.

If only partial measurements are available, one can choose the parameter `nset` in `ana_u1mu.f` or `sfana_u1mu.f`, which is preset to `nset = nrpt`, smaller than `nrpt`.

3.3.2. Reweighting to the canonical ensemble

The analysis programs are reweighting to the canonical ensemble. The simulation is performed with $\exp(\text{wln}(E))$ weights, which need to be replaced by the Boltzmann factor $\exp(-\beta E)$. Given a set of N multicanonical configurations the estimator for an observable O in the canonical ensemble is

$$\langle O \rangle(\beta) = \frac{\sum_{i=1}^N O_i \exp(-\beta E_i - \text{wln}(E_i))}{\sum_{i=1}^N \exp(-\beta E_i - \text{wln}(E_i))}. \quad (44)$$

Eq. (44) involves large terms in the numerator and denominator that can cause an overflow. To avoid this we use logarithmic coding as described in [14]. Instead of adding two numbers one expresses the logarithm of the sum through their logarithms. With this strategy one effectively evaluates the logarithm of the numerator and denominator, which are of the same order, and exponentiates the difference.

The `u1_ts_zln.f` subroutine performs the reweighting of the time series to a given value of β according to Eq. (44). Since the reweighting procedure is non-linear, one expects a bias, which is for `nrpt` patches proportional to $\tau_{\text{int}}/(\text{nmeas} * \text{nsW})$. Using jackknife error bars the bias becomes reduced by a factor $1/(\text{nrpt}-1)$. This is realized by the `u1_ts_zlnj.f` subroutine. If one is not yet satisfied, one can go on and use the jackknife approach to estimate the bias explicitly.

3.4. Example runs

We have prepared MUCA example runs in the subfolders

`MUCA3D04t06xb2p0` and `MUCA4D04t06xb1p1`

of the folder `ExampleRuns`. The values of `actmin` and `actmax` in `u1muca.par` are estimates from the previously discussed short canonical runs. The last four characters in the subfolder names denote the value of `beta_table` for which the BMHA table is calculated.

The `*.d` test files left in these subfolders were obtained from the analysis of MUCA data obtained by the preset runs. The MUCA data themselves are produced in `*.D` files, which have been removed, because they are unformatted and readability is only guaranteed on the platform on which they are produced. The MUCA data production goes through three steps of individual runs. First one has to compile and run the program `u1wl_bmho.f`, which uses our WL recursion to obtain a working estimate of the MUCA weights. Subsequently two runs of MUCA data production are performed by the program `u1mu_bmho.f`. After each data production step one may execute the data analysis programs `ana_u1mu.f` and `sfana_u1mu.f`.

In our examples the WL recursion is considered complete after 20 successful recursion steps (31). In 3D this was achieved after 22 cycling (tunneling) events. In 4D 23 cycling events were needed. Then, during the simulation with fixed weights, more than 1000 tunnelings per job were recorded in 3D. In 4D 214 tunnelings occurred in the first and 247 in the second MUCA run. These numbers vary across different platforms. The results of the analysis programs are shown in Fig. 3 for the specific heat, Fig. 4 and 5 for the susceptibilities and in Fig. 6 for the first three non-trivial structure factors. On our 2 GHz PC the data production took 74m per job. Before, the WL recursion completed in just 2m27s.

In 3D the specific heat does not diverge and the transition is much broader. We show in Fig. 7 the Polyakov susceptibility. On our PC the WL recursion completed in 6s and the data production took 7m3s per job.

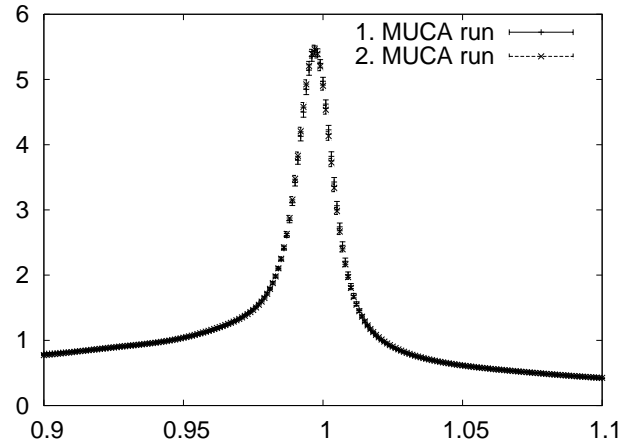


Figure 3: Specific heat on a $6^3 4$ lattice.

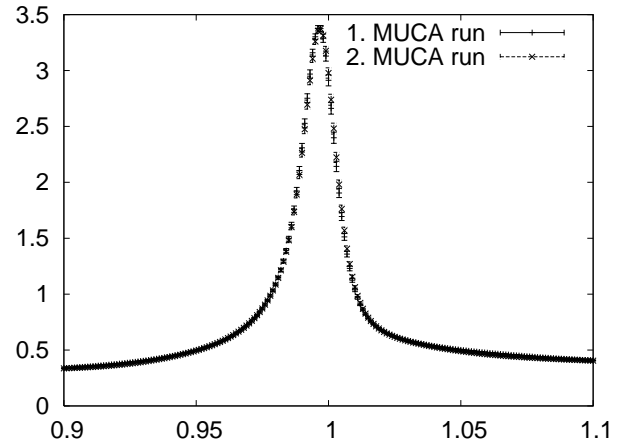


Figure 4: Polyakov loop susceptibility on a $6^3 4$ lattice.

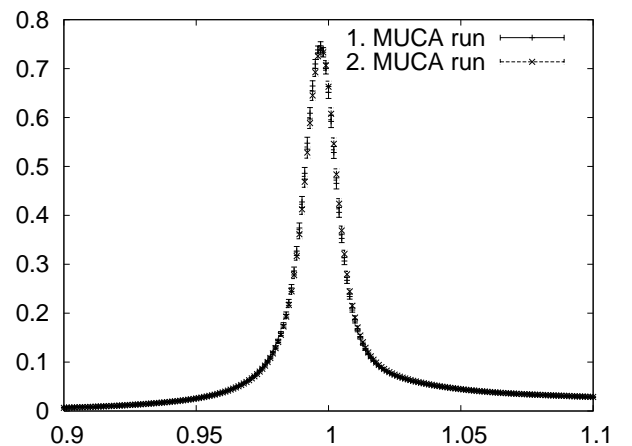


Figure 5: Polyakov loop susceptibility with respect to β on a $6^3 4$ lattice.

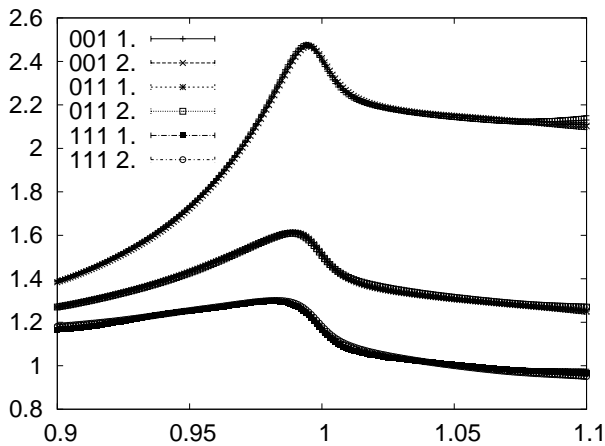


Figure 6: Structure factors on a $6^3 4$ lattice (1. and 2. MUCA runs).

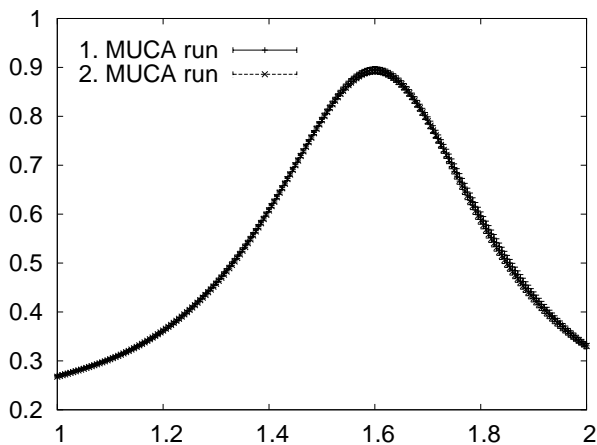


Figure 7: Polyakov loop susceptibility on a $6^2 4$ lattice.

4. Summary and Conclusions

We think that the open source Fortran code documented in this paper can be modified for many applications in statistical physics and LGT, considerably beyond the U(1) gauge group. A number of parameters can be varied, but one should have in mind that most of them have not been tested. Obviously, it is in the responsibility of the user to perform rigid tests and verifications before trusting any of the result.

Acknowledgments

This work was in part supported by the U.S. Department of Energy under contracts DE-FG02-97ER41022, DE-FC02-06ER-41439 and NSF grant 0555397.

References

- [1] H. Rothe, *Lattice Gauge Theories: An Introduction*, World Scientific, Singapore, 2005.
- [2] K. Wilson, Confinement of quarks, *Phys. Rev. D* 10 (1974) 2445–2459.

- [3] J. Jersak, T. Neuhaus, P. Zerwas, U(1) lattice gauge theory near the phase transition, *Phys. Lett. B* 133 (1983) 103–107.
- [4] G. Arnold, T. Lippert, T. Neuhaus, K. Schilling, Finite size scaling analysis of compact QED, *Nucl. Phys. B (Proc. Suppl.)* 94 (2001) 651–656.
- [5] G. Arnold, B. Bunk, T. Lippert, K. Schilling, Compact QED under scrutiny: it's first order, *Nucl. Phys. B (Proc. Suppl.)* 119 (2001) 864–866.
- [6] M. Vettorazzo, P. de Forcrand, Electromagnetic fluxes, monopoles and the order of 4d compact U(1) phase transition, *Nucl. Phys. B* 686 (2004) 85–118.
- [7] B. Berg, A. Bazavov, Non-perturbative U(1) gauge theory at finite temperature, *Phys. Rev. D* 74 (2006) 094502.
- [8] A. M. Polyakov, Quark Confinement and Topology of Gauge Groups, *Nucl. Phys. B* 120 (1977) 429–458.
- [9] M. Gopfert, G. Mack, Proof of Confinement of Static Quarks in Three-Dimensional U(1) Lattice Gauge Theory for All Values of the Coupling Constant, *Commun. Math. Phys.* 82 (1981) 545.
- [10] V. L. Berezinsky, Destruction of long range order in one-dimensional and two-dimensional systems having a continuous symmetry group. 1. Classical systems, *Sov. Phys. JETP* 32 (1971) 493–500.
- [11] J. M. Kosterlitz, D. J. Thouless, Ordering, metastability and phase transitions in two-dimensional systems, *J. Phys. C* 6 (1973) 1181–1203.
- [12] O. Borisenko, M. Gravina, A. Papa, Deconfinement transition in the compact 3d U(1) lattice gauge theory at finite temperatures, *J. Stat. Mech.* 2008 (2008) P08009.
- [13] B. Berg, T. Neuhaus, Multicanonical algorithms for first order phase transitions, *Phys. Lett. B* 267 (1991) 249–253.
- [14] B. Berg, *Markov Chain Monte Carlo Simulations and Their Statistical Analysis*, World Scientific, Singapore, 2004.
- [15] F. Wang, D. Landau, Efficient, multiple-range random walk algorithm to calculate the density of states, *Phys. Rev. Lett.* 86 (2001) 2050–2053.
- [16] A. Bazavov, B. Berg, Heat bath efficiency with a Metropolis-type updating, *Phys. Rev. D* 71 (2005) 114506.
- [17] S. Adler, Over-relaxation method for the Monte Carlo evaluation of the partition function for multiquadratic actions, *Phys. Rev. D* 23 (1981) 2901–2904.
- [18] N. Metropolis, A. Rosenbluth, N. Rosenbluth, A. Teller, E. Teller, Equation of state calculations by fast computing machines, *J. Chem. Phys.* 21 (1953) 1087–1092.
- [19] R. Wensley, Monopoles and U(1) lattice gauge theory, PhD dissertation, University of Illinois at Urbana-Champaign, Department of Physics, ILL-TH-89-25 (1989).
- [20] T. Hattori, H. Nakajima, Improvement of efficiency in generating random U(1) variables with Boltzmann distribution in Monte Carlo calculations, *Nucl. Phys. B (Proc. Suppl.)* 26 (1992) 635–637.
- [21] W. Hastings, Monte Carlo sampling methods using Markov chains and their applications, *Biometrika* 57 (1970) 97–109.
- [22] S. Adler, Overrelaxation algorithms for lattice field theories, *Phys. Rev. D* 37 (1988) 458–471.
- [23] M. Creutz, Overrelaxation and Monte Carlo simulation, *Phys. Rev. D* 36 (1987) 515–519.
- [24] A. Bazavov, B. Berg, S. Dubey, Phase transition properties of 3D Potts models, *Nucl. Phys. B* 802 (2008) 421–434.
- [25] B. Berg, W. Janke, Wang-Landau multibondic simulations for second-order phase transition, *Phys. Rev. Lett.* 98 (2007) 040602.
- [26] W. Yang, et al., Quantitative computer simulations of biomolecules: A snapshot, *J. Comp. Chem.* 129 (2008) 668–672.